Electronic Supplementary Material (ESI) for Organic Chemistry Frontiers.

A redox-responsive supramolecular amphiphile fabricated by selenium-containing pillar[5]arene-based host–guest recognition

Yujuan Zhou, Kecheng Jie and Feihe Huang*

State Key Laboratory of Chemical Engineering, Center for Chemistry of High-Performance & Novel Materials, Department of Chemistry, Zhejiang University, Hangzhou 310027, P. R. China; Fax and Tel: +86-571-8795-3189; Email address: fhuang@zju.edu.cn.

Electronic Supplementary Information (16 pages)

1. Materials and methods

All reagents were commercially available and used as supplied without further purification. Solvents were either employed as purchased or dried according to procedures described in the literature. **H1**,[S1] **H2**,[S1] and **G1**[S2] were prepared according to published procedures. ^{1}H NMR and ^{13}C HMR spectra were recorded with a Bruker Avance DMX 400 spectrophotometer or Bruker Avance DMX 500 using the deuterated solvent as the lock and the residual solvent or TMS as the internal reference. Transmission electron microscopy (TEM) investigations were carried out on a HITACHI HT-7700 instrument. Scanning electron microscopy (SEM) investigations were carried out on a JEOL 6390LV instrument. Dynamic light scattering (DLS) was carried out on a Malvern Nanosizer S instrument at room temperature. Isothermal titration calorimetry (ITC) experiment was performed on a VP-ITC micro-calorimeter (Microcal, USA). Mass spectra were obtained on a Bruker Esquire 3000 plus mass spectrometer (Bruker-Franzen Analytik GmbH Bremen, Germany) equipped with an ESI interface and an ion trap analyzer. Elemental analysis were carried out on a varioMICRO V 1.9.5 instrument. Atomic force microscopy (AFM) experiments were performed on a Multi-Mode Nanoscope-IIIa Scanning Probe Microscope (Veeco Company, USA) in the tapping mode. MALDI-TOF mass spectrometry was performed on a Bruker UltrafleXtreme instrument. Elemental analysis were carried out on a varioMICRO V 1.9.5 instrument.

*2. Synthesis of guest **G2***

Scheme S2. Synthetic route to **G2**.

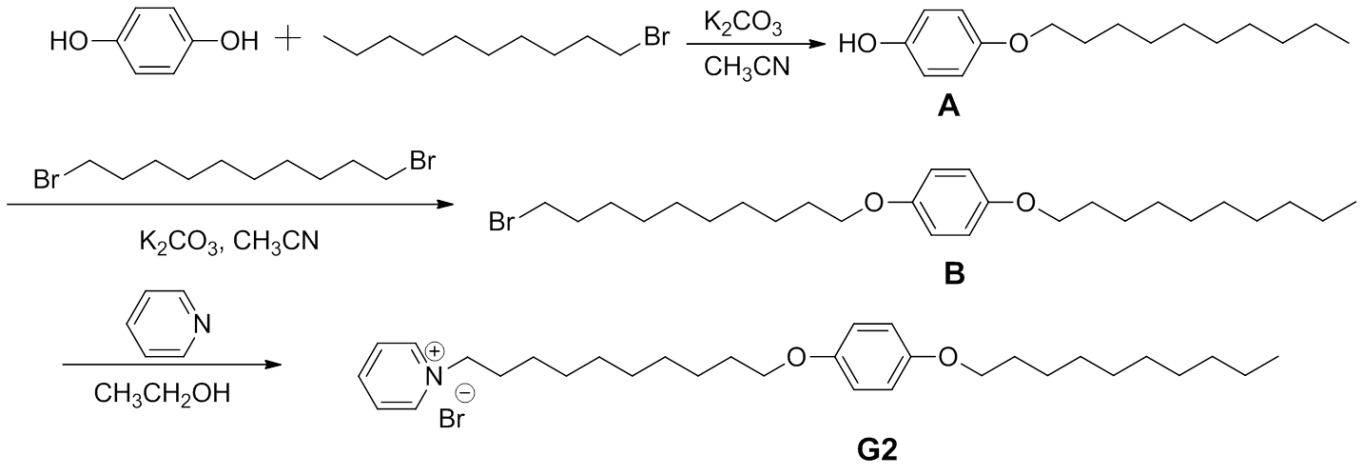

*2.1 Synthesis of **A***

K_2CO_3 (33.1 g, 240 mmol) and 1-bromodecane (39.6 g, 180 mmol) were added to a solution of hydroquinone (6.60 g, 60.0 mmol) in MeCN (300 mL). The reaction mixture was stirred at reflux for 24 hours. After the solid was filtered off, the filtrate was evaporated under vacuum, and the residue was purified by flash column chromatography on silica gel (dichloromethane/petroleum ether = 2:1, *v*/*v*) to afford **A** (8.00 g, 53.0%) as a white solid.[S3] The proton NMR spectrum of **A** is shown in Fig. S1. ^{1}H NMR (400 MHz, $CDCl_3$, 298 K) δ (ppm): 6.80–6.74 (m, 4H), 3.89 (t, J = 12 Hz, 2H), 1.78–1.71 (m, 2H), 1.45–1.40 (m, 2H), 1.30 (m, 12H), 0.88 (t, J = 16 Hz, 3H). The ^{13}C NMR spectrum of **A** is shown in Fig. S2. The ^{13}C NMR (100 MHz, $CDCl_3$, 298 K) δ (ppm): 153.33, 149.33, 116.10, 115.99, 115.62, 68.75, 31.92, 29.61, 29.58, 29.44, 29.39, 29.35, 26.07, 22.71, 14.15. LRESIMS is shown in Fig. S3: *m*/*z* 249.0 $[\mathbf{A} - H]^-$.

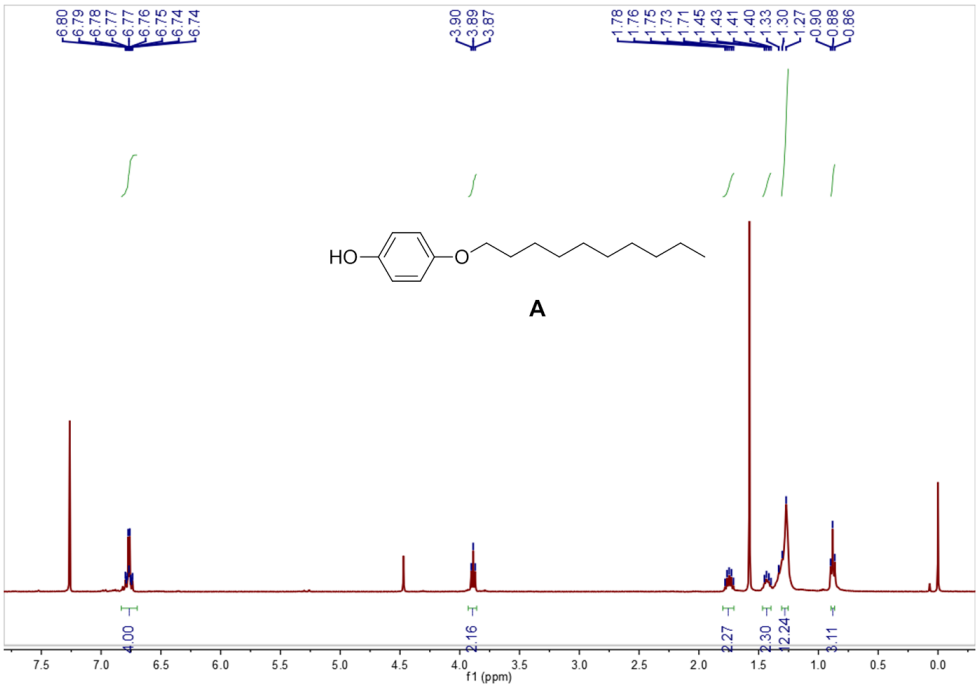

Fig. S1 ^{1}H NMR spectrum (400 MHz, chloroform-*d*, 298 K) of **A**.

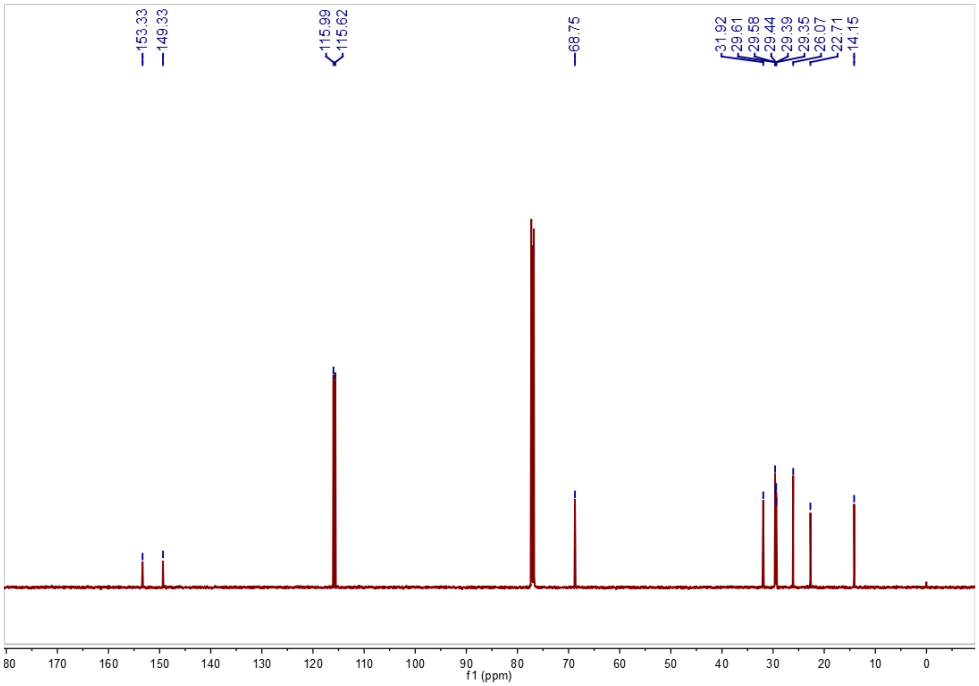

Fig. S2 ^{13}C NMR spectrum (100 MHz, chloroform-*d*, 293 K) of **A**.

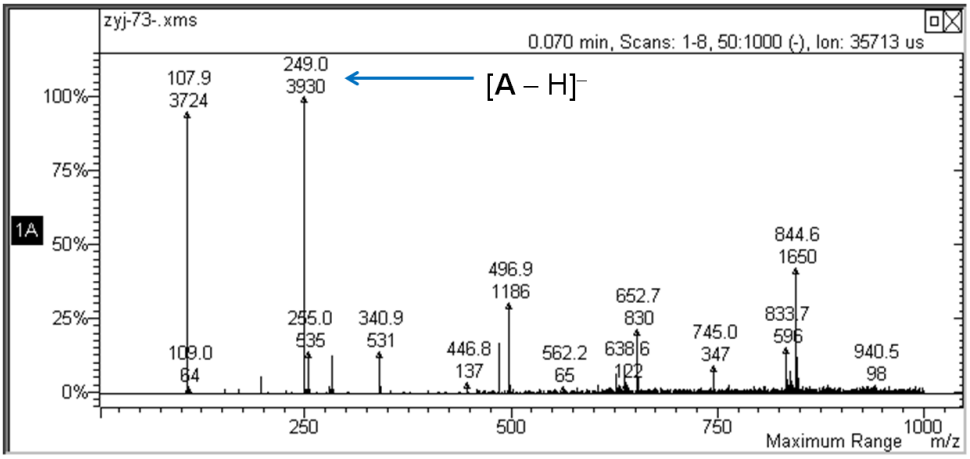

Fig. S3 Electrospray ionization mass spectra of **A**. Assignment of the main peak: *m*/*z* 249.0 [**A** – H]$^-$.

*2.2 Synthesis of **B***

K_2CO_3 (3.31 g, 24.0 mmol) and 1-bromodecane (3.96 g, 18.0 mmol) were added to a solution of **A** (1.50 g, 6.00 mmol) in MeCN (300 mL). The reaction mixture was stirred at reflux for 12 hours. After the solid was filtered off, the solvent was cooled to room temperature. The precipitated product **B** was collected by filtration, washed with petroleum ether and dried under vacuum as a white solid (1.90 g, 67.5%).[S3] The proton NMR spectrum of **B** is shown in Fig. S4. ^{1}H NMR (400 MHz, $CDCl_3$, 298 K) δ (ppm): 6.82 (s, 4H), 3.89 (t, J = 12 Hz, 4H), 3.41 (t, J = 16 Hz, 2H), 1.87–1.71 (m, 6H), 1.44–1.27 (m, 26H), 0.88 (t, J = 16 Hz, 3H). The ^{13}C NMR spectrum of **B** is shown in Fig. S5. The ^{13}C NMR (100 MHz, $CDCl_3$, 298 K) δ (ppm): 153.20, 153.17, 115.38, 68.67, 68.62, 34.10, 32.84, 31.92, 29.61, 29.59, 29.46, 29.40, 29.37, 29.35, 28.76, 28.18, 26.08, 26.05, 22.91, 14.15. LRESIMS is shown in Fig. S6: *m*/*z* 485.3 [**B** + OH^-]$^-$.

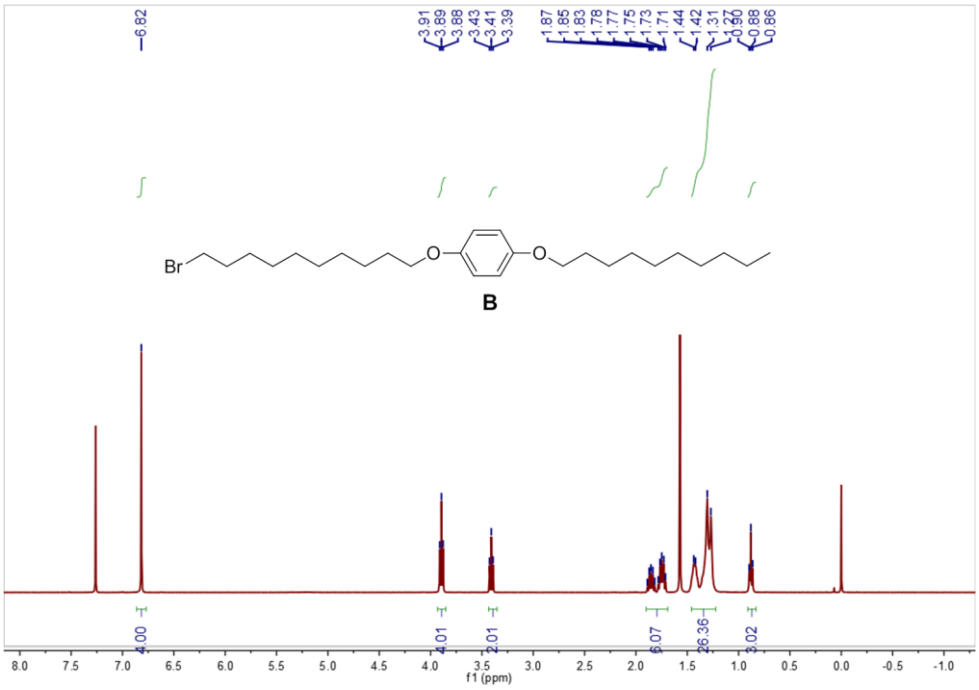

Fig. S4 ^{1}H NMR spectrum (400 MHz, chloroform-*d*, 298 K) of **B**.

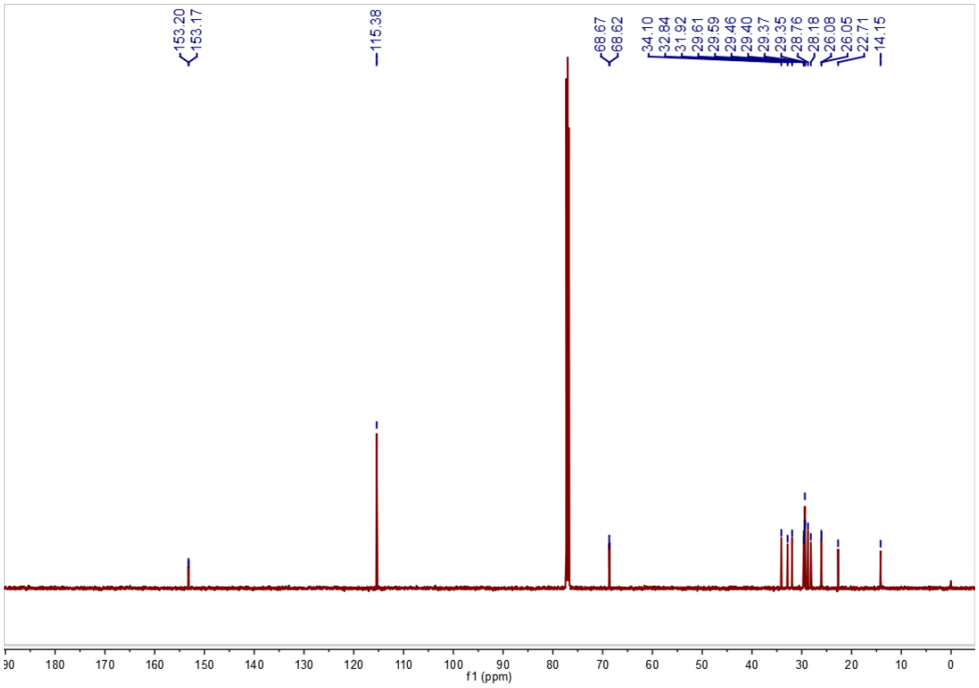

Fig. S5 ^{13}C NMR spectrum (100 MHz, chloroform-*d*, 293 K) of **B**.

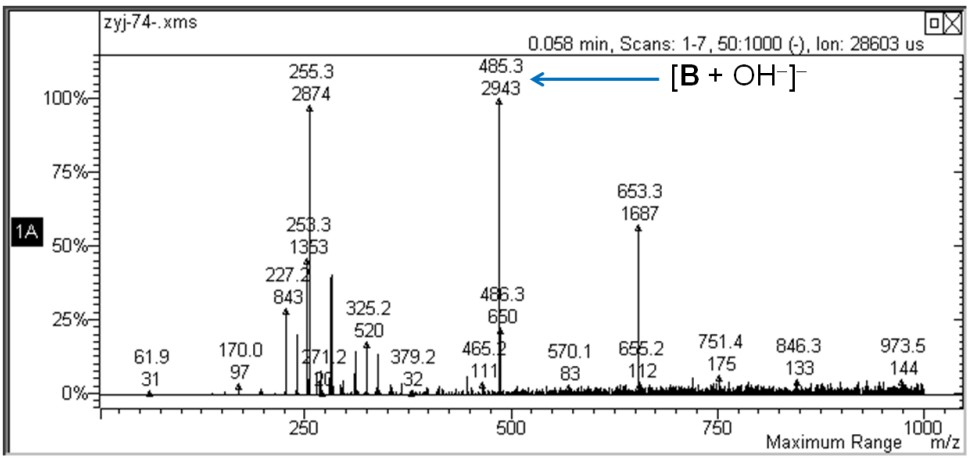

Fig. S6 Electrospray ionization mass spectra of **B**. Assignment of the main peak: *m*/*z* 485.3 [**B** + OH^-]$^-$.

2.3 Synthesis of ***G2***[S4]

B (0.469 g, 1.00 mmol) was added to a solution of pyridine (0.158 g, 2.00 mmol) in ethyl alcohol (100 mL). The reaction mixture was stirred at reflux for 24 hours. After the solvent was removed, the solid was washed twice with diethyl ether (200 mL) to afford **G2** (0.400 g, 85.5%) as a pale yellow solid. Mp 98.5–98.7 ºC. The proton NMR spectrum of **G2** is shown in Fig. S7. ^{1}H NMR (400 MHz, $CDCl_3$, 298 K) δ (ppm): 9.44 (d, J = 4 Hz, 2H), 8.47 (t, J = 12 Hz, 1H), 8.10 (t, J = 8 Hz, 2H), 6.80 (s, 4H), 5.01 (t, J = 12 Hz, 2H), 3.89–3.87 (m, 4H), 2.03 (t, J = 12 Hz, 2H), 1.75–1.71 (m, 4H), 1.44–1.24 (m, 26H), 0.87 (t, J = 8 Hz, 3H). The ^{13}C NMR spectrum of **G2** is shown in Fig. S8. The ^{13}C NMR (100 MHz, $CDCl_3$, 298 K) δ (ppm): 153.19, 153.14, 145.12, 128.43, 115.39, 115.38, 68.68, 68.60, 62.18, 32.00, 31.90, 29.60, 29.57, 29.43, 29.41, 29.37, 29.33, 29.29, 29.23, 29.01, 26.07, 26.03, 26.00, 22.69, 14.14. LRESIMS is shown in Fig. S9: *m*/*z* 468.3 [**G2** – Br]$^+$. Anal. Calcd for $C_{31}H_{50}BrNO_2$: C, 67.86; H, 9.19; N, 2.55. Found: C, 67.84; H, 9.21; N, 2.51.

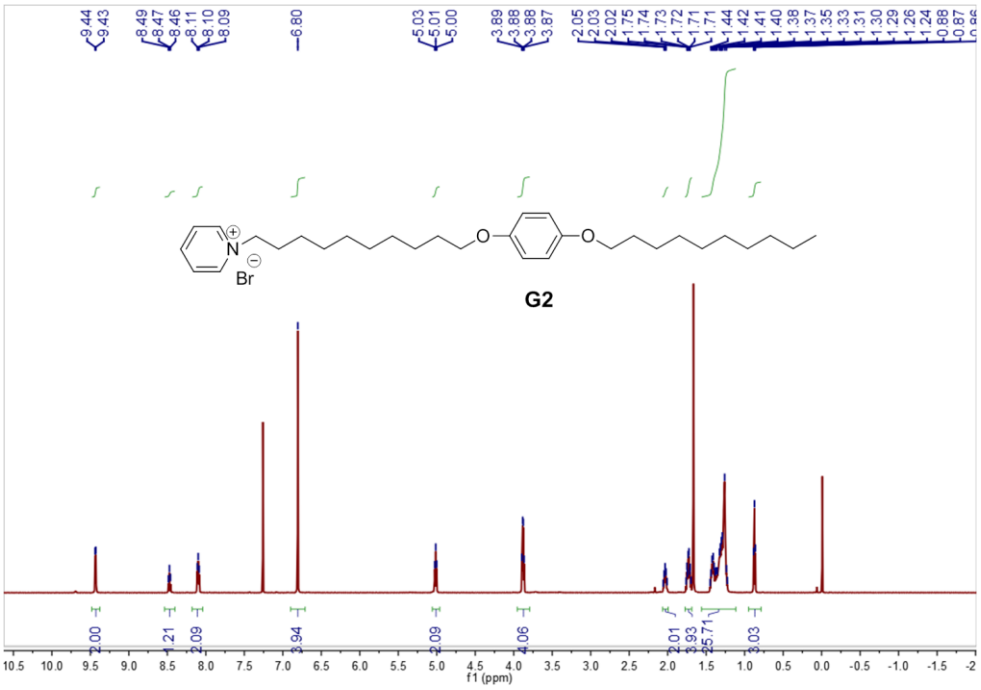

Fig. S7 ^{1}H NMR spectrum (400 MHz, chloroform-*d*, 298 K) of **G2**.

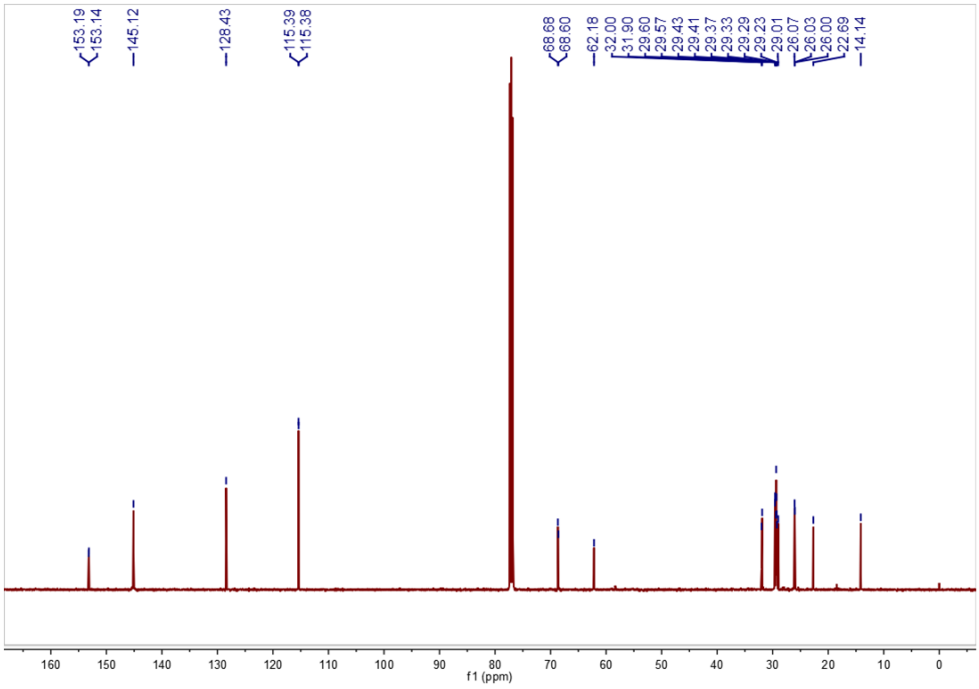

Fig. S8 ^{13}C NMR spectrum (100 MHz, chloroform-*d*, 293 K) of **G2**.

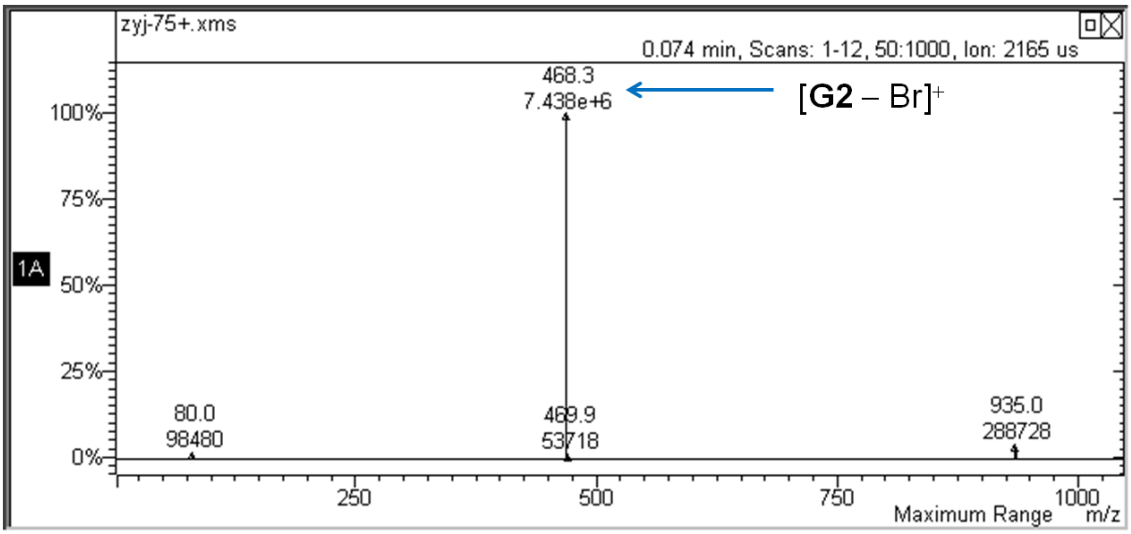

Fig. S9 Electrospray ionization mass spectra of **G2**. Assignment of the main peak: *m*/*z* 468.3 [**G2** – Br]$^+$.

*3. Host–guest complexation between **H1** and **G1***

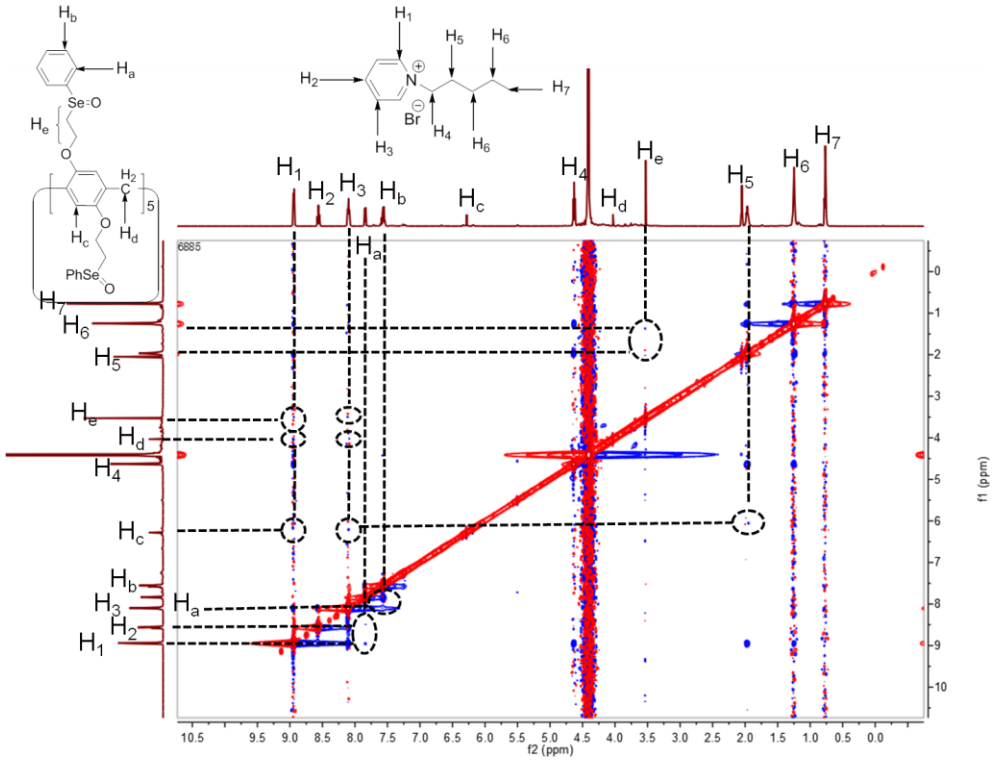

Fig. S10 2D NOESY spectrum (500 MHz, D_2O, 293 K) of **H1** (10.0 mM) and **G1** (10.0 mM).

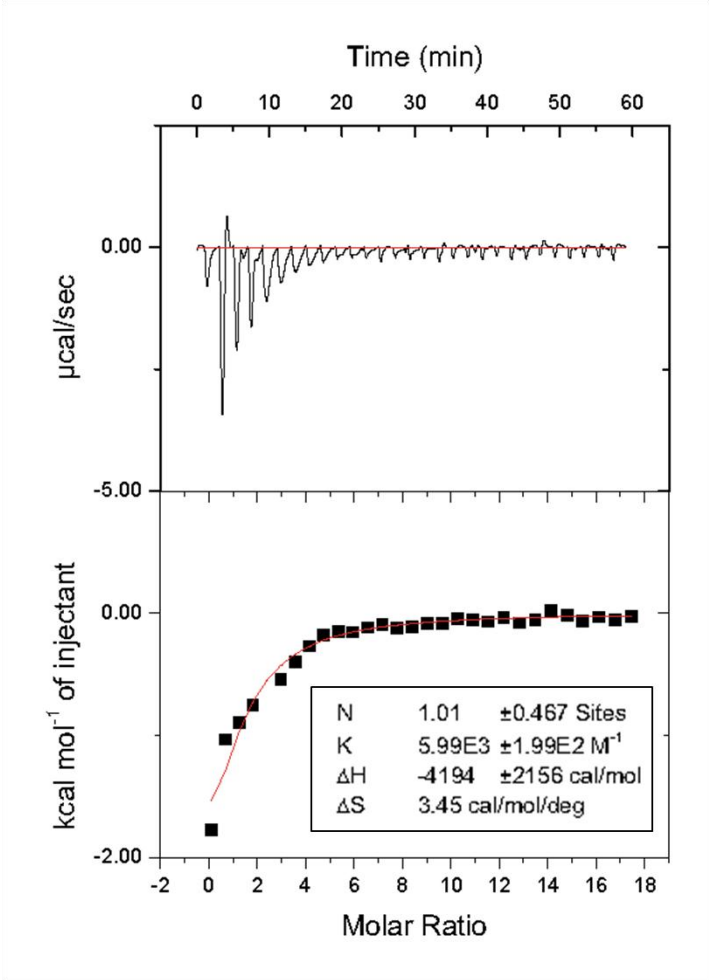

Fig. S11 Microcalorimetric titration of **G1** with **H1** in water at 298 K. (Top) Raw ITC data for 29 sequential injections (10.0 µL per injection) of a **G1** solution (2.00 mM) into a **H1** solution (0.100 mM). (Bottom) Net reaction heat obtained from the integration of the calorimetric traces.

*4. Critical aggregation concentration (CAC) determination of **G2***

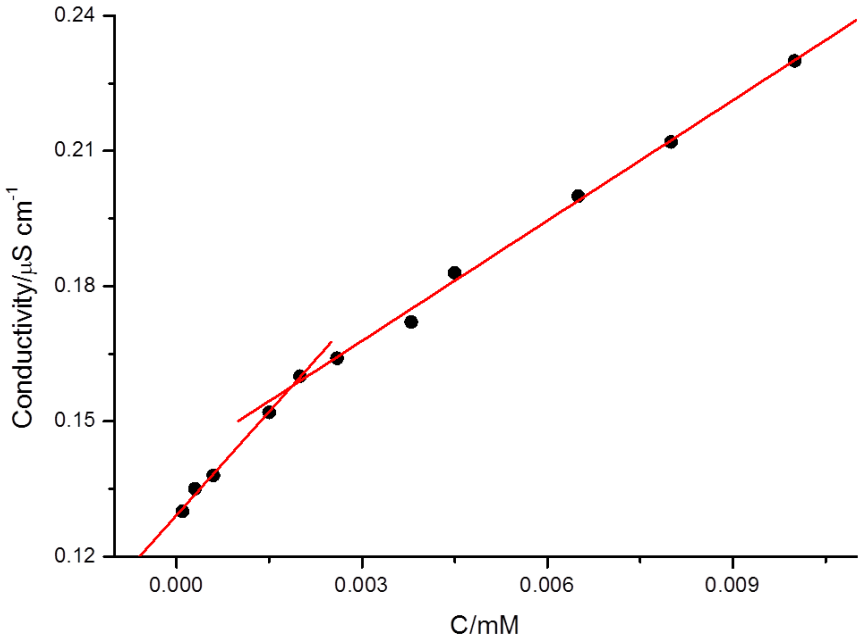

Fig. S12 The concentration-dependent conductivity of **G2** in water. The critical aggregation concentration was determined to be 1.90 × 10^{-6} M.

*5. DLS results of **G2** and **H1⊃G2***

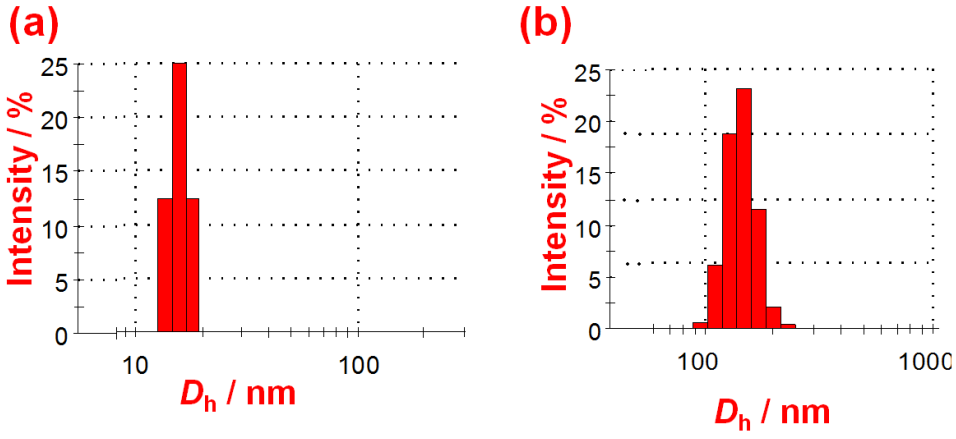

Fig. S13 (a) DLS data of **G2** (5.00 × 10^{-4} M); (b) DLS data of **H1⊃G2** (1.00 × 10^{-4} M).

*6. Critical aggregation concentration (CAC) determination of **H1⊃G2***

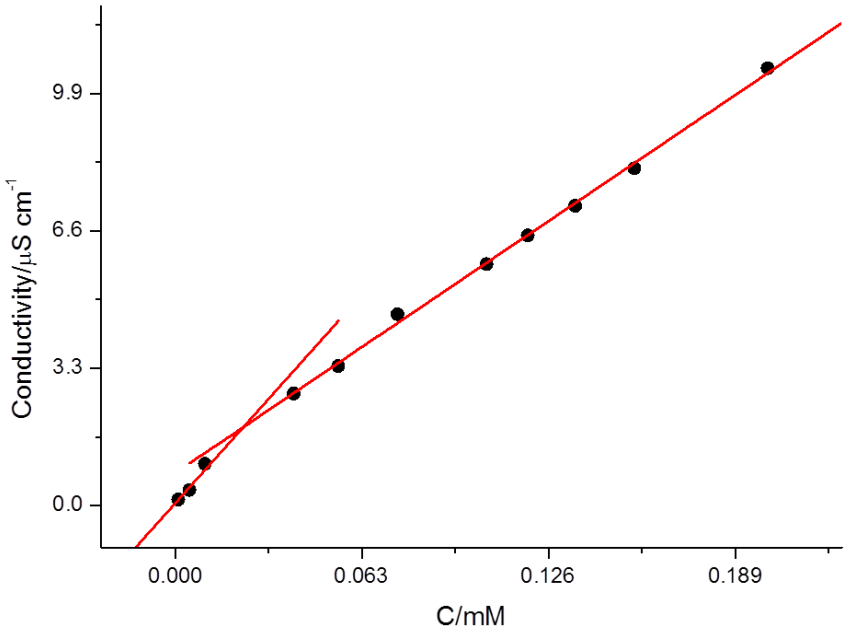

Fig. S14 The concentration-dependent conductivity of **H1⊃G2** in water. The critical aggregation concentration was determined to be 2.38 × 10^{-5} M.

*7. Enlarged TEM of **H1⊃G2***

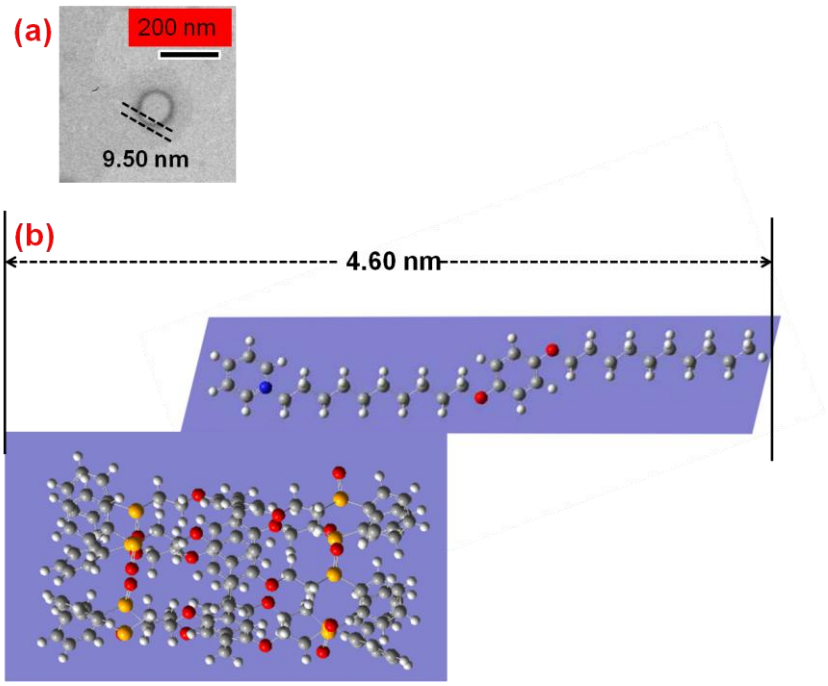

Fig. S15 (a) Enlarged TEM image of **H1⊃G2** aggregation; (b) the energy-minimized structure of **H1⊃G2** (ball and stick mode: side view) obtained from Gaussian (Gaussview V 5.0.8.0).

*8. AFM result of **H1⊃G2***

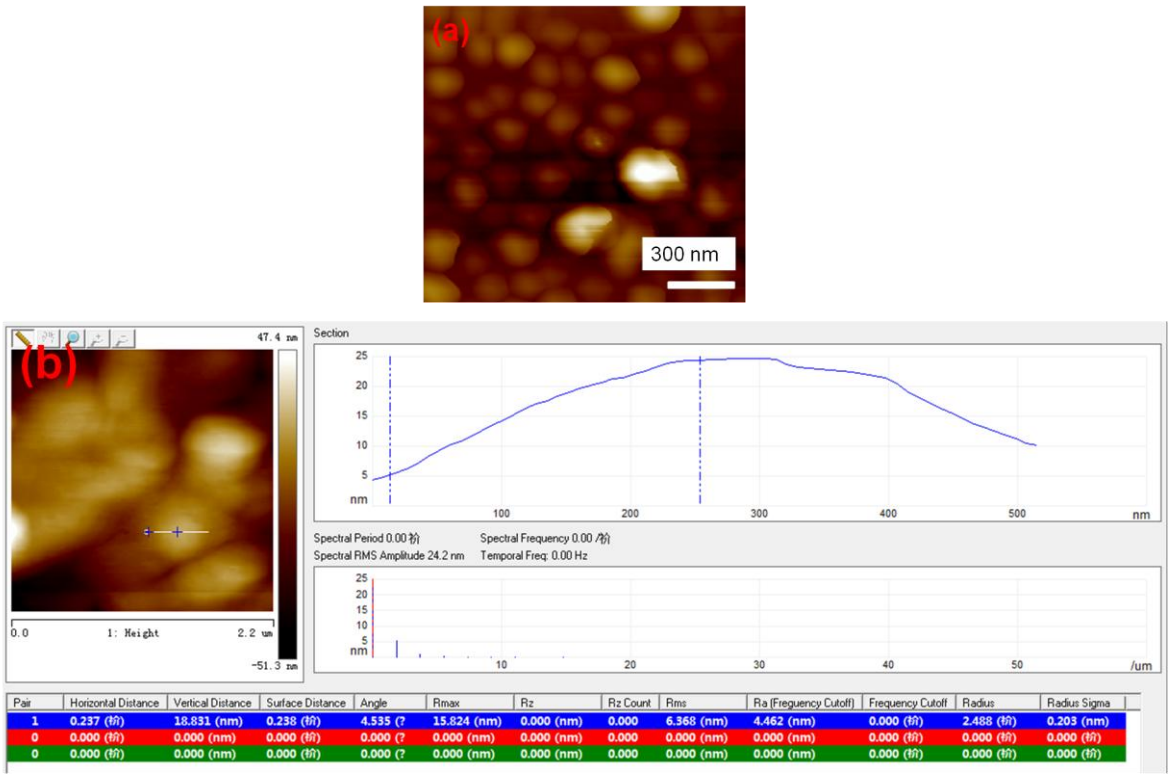

Fig. S16 (a) AFM result of the self-assembled vesicles; (b) the height measured from the AFM experiment is the height of two walls of the vesicles. It means that the wall thickness of the vesicles is 9.42 nm, which is equal to half of the vertical distance, 18.831 nm.

*9. DLS results of **H1⊃G2** after addding vatimin C and then H_2O_2*

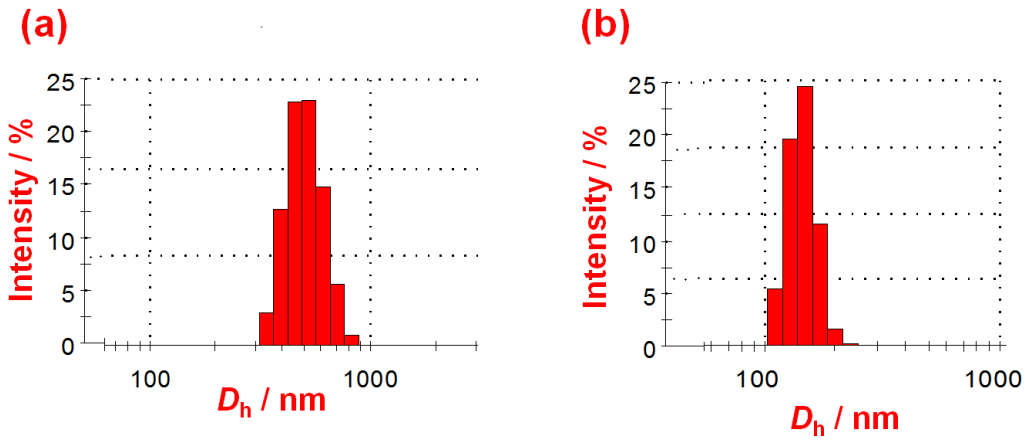

Fig. S17 (a) DLS data of **H1⊃G2** (1.00×10^{-4} M) after adding vitamin C (12 molar equiv.); (b) DLS data of a after further adding H_2O_2 (15 molar equiv.).

10. UV−vis absorption spectra of vesicles, DOX·HCl, and DOX·HCl-loaded vesicles at 25 ℃ in water

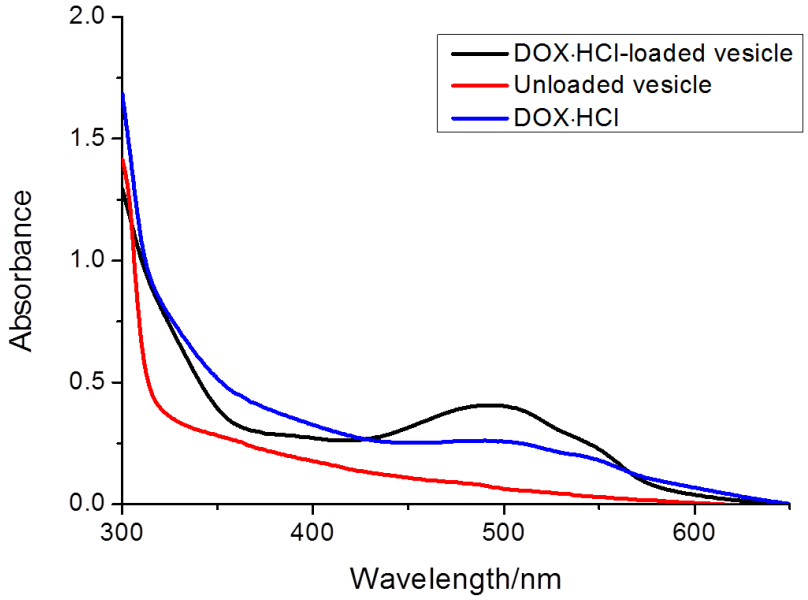

Fig. S18 UV−vis absorption spectra of vesicles, DOX·HCl, and DOX·HCl-loaded vesicles in water.

11. Loading and triggered release experiments of DOX·HCl

DOX·HCl loading experiment: DOX·HCl-loaded vesicles were prepared by adding a certain amount of DOX·HCl into a freshly prepared aqueous solution of **H1** and **G2** (2.50×10^{-4} M). The ultimate concentrations of DOX·HCl, **H1**, and **G2** were 0.050, 0.25, and 0.25 mM, respectively. The DOX·HCl-loaded vesicles were purified by dialysis (molecular weight cutoff = 3500) in distilled water for several times until the water outside the dialysis tube exhibited negligible DOX·HCl fluorescence. As a result, DOX·HCl was successfully loaded into the vesicles constructed from **1**.

The DOX·HCl encapsulation and loading efficiency were calculated by the following equations:

Encapsulation Efficiency (%) = ($m_{\text{DOX·HCl -loaded}}$ / $m_{\text{DOX·HCl}}$)100

Loading EffIciency(%) = ($m_{\text{DOX·HCl -loaded}}$/$m_{\text{vesicles}}$)100

Here $m_{\text{DOX·HCl -loaded}}$, $m_{\text{DOX·HCl}}$ and m_{vesicles} are mass values of DOX·HCl encapsulated in vesicles, DOX·HCl added, and DOX·HCl-loaded vesicles, respectively. The mass of DOX·HCl was measured by a UV spectrophotometer at 490 nm and calculated relative to a standard calibration curve in the concentrations from 5.00×10^{-3} to 2.50×10^{-2} mM in water. 2.00 mL of DOX·HCl-loaded assemblies in a dialysis bag were added into 18.0 mL of water. At predetermined time intervals, 2.00 mL of the solution outside the dialysis tube were collected and replaced by 2.00 mL of fresh water. The concentration of DOX·HCl was determined by measuring the UV absorbance at 490 nm.

12. Controlled release of DOX·HCl molecules

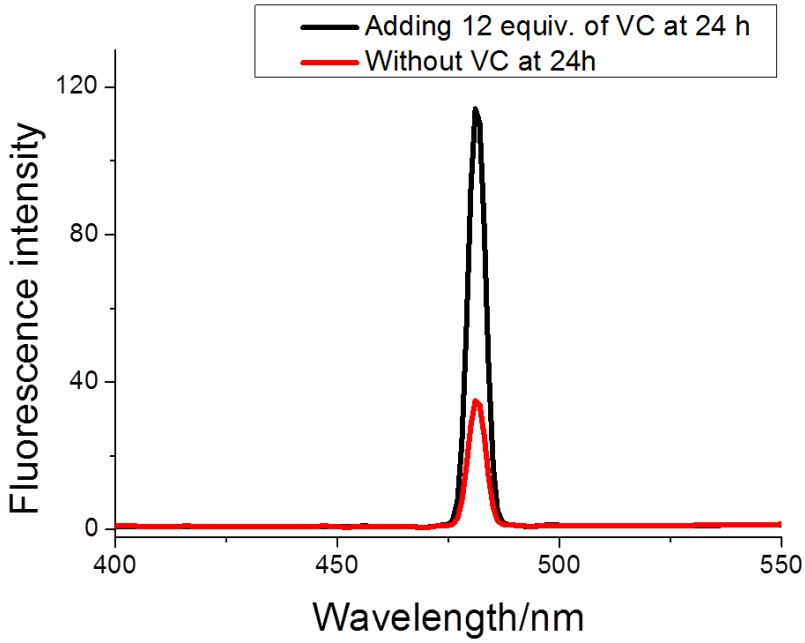

Fig. S19 Fluorescence emission spectra of DOX·HCl encapsulated in a solution of **H1** (1.00 mM) and **G2** (1.00 mM) with 12 equiv. of vitamin C or without vitamin C.

References

S1. Y. Zhou, K. Jie and F. Huang, *Chem. Commun.*, 2017, DOI: 10.1039/C7CC04779G.

S2 Z. He, G. Ye and W. Jiang, *Chem. Eur. J.*, 2015, **21**, 3005.

S3 K. Tahara, K. Katayama, M. O. Blunt, K. Iritani, S. D. Feyter, Y. Tobe, *ACS Nano*, 2014, **8**, 8683.

S4 D. Haristoy and D. Tsiourvas, *Chem. Mater.*, 2003, **15**, 2079